

# An Optimized Electrifying Strategy for the Permanent-Magnet Spherical Actuator Based on the Cuckoo Algorithm

Xiwen Guo<sup>1,2,3</sup>, Siao Wu<sup>1,2</sup>, Qunjing Wang<sup>1,2,4</sup>, Guoli Li<sup>1,2,3</sup>, Yan Wen<sup>1,2</sup>

<sup>1</sup> School of Electrical Engineering and Automation, Anhui University, Hefei, Anhui, China

<sup>2</sup> National Engineering Laboratory of Energy-saving Motor & Control Technique, Anhui University, Anhui, China

<sup>3</sup> Industrial Power Saving and Safety Laboratory, Anhui University, Hefei, Anhui, China

<sup>4</sup> Collaborative Innovation Centre of Industrial Energy-Saving and Power Quality Control, Anhui University, China  
E-mail: wsa0102@163.com

**Abstract.** To assure a complex control of the permanent-magnet spherical actuator (PMSA), an optimized electrifying strategy based on the cuckoo algorithm is proposed. An electromagnetic analysis in mode and the PMSA torque values of the rotor and stator coils of different angles are obtained. A position-torque black-box model is set-up using the random forest method. Combined with the spin and tilt trajectory, the cuckoo algorithm optimizes the electrifying strategy resulting in a 5% ~ 18% power-loss reduction. Simulations and experiment show that by using the proposed strategy, the PMSA control system ensure a stable and effective performance of a reduced power-loss rate, thus providing a reference for the PMSM high-precision trajectory tracking control.

**Keywords:** Permanent-Magnet Spherical Actuator (PMSA); Random Forest; Cuckoo Algorithm; Electrifying Strategy

## Algoritem za krmiljenje sferičnega pogona s trajnim magnetom

V članku je predstavljen algoritem za krmiljenje sferičnega pogona s trajnim magnetom. V prvem koraku smo s pomočjo elektromagnetne analize določili vrednosti navora rotorske in statorske tuljave pod različnimi koti. Nato smo s pomočjo metode naključnega gozda vzpostavili model za nastavitev navora. Na osnovi teh vrednosti smo z upoštevanjem smeri vrtenja in nagiba optimizirali krmiljenje, ki zmanjša izgubo moči za 5 do 18 %. Eksperimentalni rezultati kažejo, da lahko s predlagano metodo zagotovimo stabilno in učinkovito delovanje z manjšo izgubo moči.

## 1 INTRODUCTION

Because the spherical actuator (SA) can realize a multi-degree-of-freedom (DOF) motion, and has the advantages of a small volume, light weight and fast response speed, it can solve the problems of a large volume, slow response speed and low positioning accuracy of the traditional multi-DOF motion device. Therefore, as a new direct actuator, SA can be used in robot joints, satellite attitude control, panoramic camera system and power-assisted wheelchair.

At present, scholars propose the DC type, variable reluctance type and other different SA structures, especially permanent-magnet actuator (PMA) because of its low loss, high efficiency and simple structure, which has been widely concerned. For PMSA, electromagnetic modeling and high-precision control

have become the main research directions. In terms of electromagnetic modeling, Li Zheng calculates the magnetic field and torque of the traditional PMSA, and proposes a simplified torque calculation model and a nonlinear system dynamics model which allopther reduce the amount of calculation [1]. In [2], a new type of a 3-DOF deflection PMA is proposed. The PMA magnetic field and torque distribution are analyzed and calculated, the rotor magnetic field is calculated and a back EMF model is set-up. In [3], Yan Liang proposes a superposition PM modeling method using the Halbach array distribution on the SA rotor. The magnetic array is divided into a radial and tangential part, and the corresponding mathematical model is presented. The scheme improves the modeling accuracy and facilitates a magnetic field analysis. In [4], a dynamic decoupling control algorithm is proposed based on a fuzzy controller and neural network identifier to improve the PMSA static and dynamic model of the control system. In [5], a robust iterative learning control algorithm is presented to improve the PMSA trajectory tracking performance. In [6-7], Liu Jingmeng proposes a dynamic decoupling control strategy and an adaptive control system combining a backstepping and synovial control, both of are advanced robustness. In [8-11], Guo Xiwen investegates the SA position tracking, complex continuous trajectory planning and power on the strategy. In [12], a new type of the stator coil is proposed. In it, the position and the rotation motion are

carried out separately which solves the complex control algorithm problem when one coil participates in both motions. In [13], Bai Kun proposes a method to realize a PMSA directional control by using a real-time measurement of the existing rotor magnetic field in the feedback loop, the obtained trajectory control results are good. In [14], Nishiura proposes a compensation method to eliminate the cogging torque to improve the controllability of the system. In [15], the motion is divided into the rotation and tilt motion and a decoupling control is adopted. In [16], Nguyen studies the control problem of a multi-DOF actuator with an uncertain torque model and unmodels the system parameters. The obtained tracking performance of the controlled rotor orientation is good. However, due to the different SA structures and large number of the stator coils, modeling is quite complex.

In recent years, some data-driven modeling and optimization schemes have been widely used in some fields [17-19]. Among them, a random forest algorithm can well handle the large data analysis method of multi-dimensional samples. Its smaller adjustment parameters, high prediction accuracy and strong generalization ability, effectively avoids the occurrence of the "over fitting" phenomenon, it is suitable for the operation of various data sets and assure a good robustness. Compared with the traditional particle swarm optimization (PSO) algorithm, simulated annealing method and ant colony algorithm, it easily to falls into a local optimization and has a large amount of calculations. The Cuckoo algorithm has fewer parameters and a faster speed. Being well combined and being strongly compatibilied with other algorithms, it is often used to solve the optimization problems [20-23].

Therefore, based on the random forest method, the PMSM torque-position information is modeled in a black box, and the cuckoo algorithm is used to optimize the power consumed by the strategy. Second 2 of this paper introduces the basic principle of the random forest. Section 3 presents the PMSA torque-position data using a virtual displacement method and set-up a PMSA torque-position black box model by using the random forest algorithm. In Section 4, the cuckoo algorithm is used to optimize the power consumed by the PMSM strategy. The results are compared with the pseudo inverse matrix (PIM) algorithm and PSO algorithm. The final data analysis shows that using the cuckoo algorithm reduces the PMSA power losses. In Section 5, the cuckoo algorithm is experimentally verified and its ability to optimize the PMSA power consumption is further verified by the error analysis of the spin and tilt motion.

## 2 BASIC PRINCIPLES OF THE RANDOM FOREST ALGORITHM

Basically, the Random forest algorithm is a variant of a bagging algorithm based on the decision tree [24-25]. It can be used to solve the classification and regression

problems. From the practical application point of view, the random forest algorithm is highly accurate for almost any kind of data prediction, and because of its own algorithm mechanism, it can directly process high-dimensional samples without reducing in dimensions.

### 2.1 Bagging sampling method

Each sample of the bagging method is obtained by sampling the net proved initial data set. It is a sampling method based on repeatable random sampling. It uses Bootstrap resampling to select the  $n$ -training samples randomly from the original sample set. The process is then cycled  $n_{\text{tree}}$ -times to get a training set. When generating the  $n_{\text{tree}}$  training subsets, each training sample can be extracted at a repeated training, there will always be some samples unextracted. The probability that a sample will not be extracted is:

$$p_0 = \left(1 - \frac{1}{n}\right)^n \quad (1)$$

where  $n$  is the total number of the samples in the initial data. When  $n$  is large enough, equation (1)

converges to  $\frac{1}{e} = 0.368$ . That indicates that about 37% of the samples will not be extracted when the sample data is large enough.

### 2.2 CART decision tree algorithm

The CART decision tree algorithm uses the binary recursive segmentation method to divide the original sample set into two subsets, so that there will be two branches on each non-leaf node. When a node splits, the splitting rules follow the principle of the minimum Gini index, The Gini probability distribution index ( $G(p)$ ) is:

$$G(p) = \sum_{k=1}^K p_k (1 - p_k) = 1 - \sum_{k=1}^K p_k^2 \quad (2)$$

where  $K$  is the total number of the characteristic samples in the node and  $p_k$  is the probability of the  $K$ -class feature sample in the node.

The Gini index of the sample set  $D(G(D))$  is:

$$G(D) = 1 - \sum_{k=1}^K \left(\frac{|C_k|}{|D|}\right)^2 \quad (3)$$

where  $C_k$  is the sample set and  $D$  is the sample subset of class  $K$ .

The Gini index divided by each point ( $G_{\text{split}}(D)$ ) is:

$$G_{\text{split}}(D) = \sum_{i=1}^2 \frac{|D_i|}{|D|} G(D_i) \quad (4)$$

where  $i = 1, 2$  and  $D_1$  and  $D_2$  are two subsets divided by  $D$ .

### 2.3 Random forest algorithm construction

Suppose the random forest is composed of a series of CART decision trees, with the following edge functions:

$$K(\mathbf{X}, \mathbf{Y}) = a_k I(h(\mathbf{X}, \theta_k) = \mathbf{Y}) - \max_{j \neq Y} a_k I(h(\mathbf{X}, \theta_k) = j) \quad (5)$$

where  $\mathbf{X}$  is the input vector at most different categories of  $J$ .  $j$  is a certain class of  $J$  categories,  $\mathbf{Y}$  is the correct classification vector,  $I$  is the indicator function and  $a_k$  is the function of the average value.

The generalization error ( $P_e$ ) of the random forest can be expressed as follows:

$$P_e = P_{X,Y}(K(\mathbf{X}, \mathbf{Y}) < 0) \quad (6)$$

where  $P_{X,Y}$  is the classification error probability function for given input variable  $X$ .

Maximum generalization error  $P_{e,\max}$  of the random forest can be expressed as follows:

$$P_{e,\max} \leq \frac{\bar{\rho}(1-s^2)}{s^2} \quad (7)$$

where  $\bar{\rho}$  is the average correlation coefficient of the decision tree and  $s$  is the average strength of the decision tree.

The algorithm flow is as follows:

Step 1. From original sample set  $D = \{X_1, X_2, \dots, X_m\}$ , the  $m$  samples are randomly selected to form a new sample set  $D$  used as a training sample of the decision tree.

Step 2. If each sample has  $M$ -features, constant  $k$  should be less than  $M$ . Each time the decision tree split growth needs to select a partition attribute, the  $k$  features are randomly selected and the Gini index is used to select the optimal partition attribute to partition the current sample.

Step 3. After the  $n$  decision trees are obtained by repeating steps 1 and 2, a random forest model is formed by using the relative majority voting method.

### 3. POSITION TORQUE MODELING BASED ON THE RANDOM FOREST ALGORITHM

PMSA is composed of a rotor ball, stator coil, stator shell and output shaft. Its basic structure is shown in Figure 1.

There are 40 permanent magnets on the rotor ball. They are divided into four layers. The angle between each two layers is  $30^\circ$  with an angle of  $36^\circ$  between the two adjacent PMs permanent magnets. There are 24 electrified coils on the stator shell. They are symmetrically distributed on the equator line of the stator spherical shell. There are 12 electrified coils in the upper and lower stator spherical shells. The angle

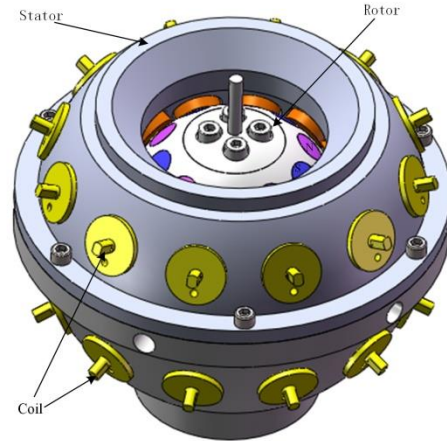


Figure 1. PMSA Structure .

between two coils is  $45^\circ$  and the coils in each layer are evenly arranged. The angle between the two coils is  $30^\circ$ . The PMSA tilt motion range is  $0-37^\circ$  and the spin range is  $0-360^\circ$ .

As there is no ferromagnetic material in PMSA, the magnetic circuit saturation can be ignored. The virtual displacement method is used to analyze the electromagnetic torque between a single stator coil and 40 permanent magnets. The PMSM model set-up based on the finite element analysis software ANSYS is shown in Figure 2.

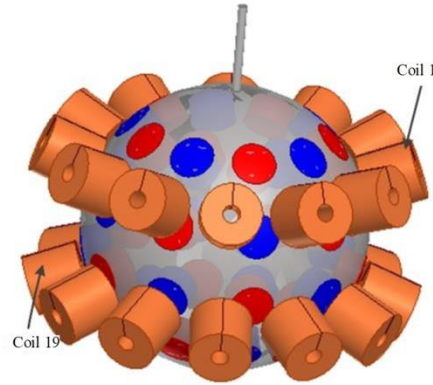


Figure 2. PMSA ANSYS model.

When there is a small displacement between the stator winding and the rotor pole, the change in the electric energy input power of the system  $\Delta W_e$  is according to the energy law equal to the sum of mechanical energy change  $\Delta W_m$  and magnetic field energy storage change  $\Delta W_f$  expressed as:

$$\Delta W_e = \Delta W_m + \Delta W_f \quad (8)$$

And hypothetically as:

$$\Delta W_f = -\Delta W_m \quad (9)$$

When a motor rotates at a small angle, the following result is obtained:

$$T = \frac{-\Delta W_m}{\Delta \theta} \quad (10)$$

For the whole magnetic-field system, the solution is:

$$\Delta W_m = \iiint_0^B \left( \int H dB \right) dv \quad (11)$$

Using the above method, the torque of 40 permanent magnets with the coil spin angle of 0-360 ° and tilt angle of 0 - 37 ° of a unit current is obtained. Due to the PMSA symmetry, the data generated by the two coils at a symmetrical position of the spherical center are the same at each position. Therefore, 12 pairs of the models are needed to use random forest method to set-up a PMSA torque model.

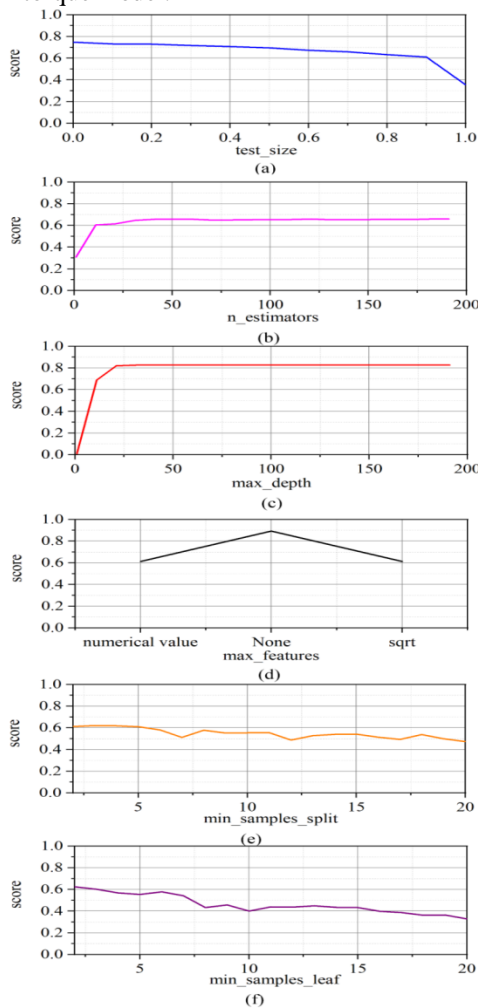


Figure 3. Learning curve of the random forest parameters.

The relationship between the position and torque is obtained by modeling the basic data obtained by the above method. The value of the initial parameter test\_size is 0.9, which means that the training set accounts for 10% of the original data. The value of the n\_estimators is 10, which represents the number of trees. The value of the max\_depth is 10, which represents the

maximum depth. The value of the max\_features is 0.1, which represents the maximum number of the features to construct the decision tree. The value of the min\_samples\_split is 2, which represents the minimum number of the samples that can be divided by the node. The value of the min\_samples\_leaf is 1, which indicates the minimum number of the samples contained in leaf nodes. According to the above parameters, the PMSA position torque model is set-up. The score of the cross validation is 0.6113. The results show that the model is not accurate sufficiently. To obtain an optimal parameter setting and create an accurate model for the next step of the research. The learning curve is studied by controlling variables. The results are shown in Figure 3.

Figure 3 (a) shows that with the increase in the value of the test\_size, the score of the model gradually decreases, and when the value is between 0 and 0.8, the score of the model changes slowly and after 0.9, the score decreases. As a larger value of the test\_size means less data to participate in training, the accuracy of the model decreases. However, if a large amount of the data is used for training to obtain a particularly good model, the time to set-up a the model reduces considerably. The results in Figure 3 (b) show that the increase in the number of the trees improves the score of the model. When the number of the trees exceeds 25, the score fluctuates around 0.65, this indicates that the impact of increasing the number of the trees is small when it exceeds a certain value, and the increase in the number of the trees also increases the modeling time. For the maximum depth, the results in Figure 3 (c) show that when the depth is between 0-25, it has a great impact on the score of the model. When the depth is above 25, the score of the model is maintained at 0.83. This indicates that the maximum depth has no impact on the random forest model when it exceeds a certain value. The results of Figure 3 (d) illustrate that when the max\_feature value is a specific value or sqrt, the score of the model will not be affected. When it is set to None, it means that there is no limit on the number of the features per tree, and the score of the model will be greatly improved. Figure 3 (e) shows the minimum number of the samples min\_samples\_split that the node can be divided learning curve between 1 and 20. A comparison, show that the score oscillation of the model decreases with the increase in the value between 1 and 20. Figure 3 (f) presents the learning curve of min\_samples\_leaf. The results show that when the value of the min\_samples\_leaf is 2, the score of the model is the highest, and when it exceeds 2, the score of the model shows a downward trend.

The study of the learning curve of the above parameters moves to verify a combination of the parameters and to obtain the optimal modeling parameters see in Table 1.

Table 1. Optimal parameters of Random Forest modeling

Basic parameters	Parameter value
test_size	0.85
n_estimators	100
max_depth	20
max_features	None
min_samples_split	3
min_samples_leaf	2

According to the value of the test\_size, the characteristic matrix samples are grouped as shown in Table 2.

Table 2. Sample division

Basic data	Training set	Test set
13718	2058	200

The position torque model is evaluated for the relationship between the position and torque, and the scores are shown in Table 3.

Table 3. Model scores

Model	Score	Model	Score
1	0.984070	7	0.982764
2	0.985754	8	0.983946
3	0.985905	9	0.985860
4	0.983570	10	0.981280
5	0.983083	11	0.983614
6	0.983875	12	0.982772

The results show that the scores of each model are above 0.98. This means that the 12 PMSA position torque models created by the random forest method are accurate and reliable.

#### 4. ELECTRIFYING STRATEGY BASED ON THE CUCKOO ALGORITHM

The Cuckoo algorithm was proposed by Yang and DEB, Cambridge scholars in 2009 [26]. It is a heuristic algorithm to simulate the cuckoo parasitic breeding. The algorithm combines the cuckoo breeding process with the Levy's flight search mode of birds.

##### 4.1 Basic principle of the cuckoo algorithm

If the position of the  $i$  nest in the first generation is expressed as  $x_i^{(t)}$ , the random search path is expressed as  $L(\lambda)$ . Then the CS algorithm nest finding path and location update formula is as follows:

$$x_i^{(t+1)} = x_i^{(t)} + \partial \oplus L(\lambda) \quad i = 1, 2, \dots \quad (12)$$

where  $\partial$  is the step size control variable,  $x_i^{(t+1)}$  is the new nest position and  $\oplus$  is the point-to-point product.

$$L(\lambda) = 0.01 \frac{\mu}{|v|^\beta} (x_i^{(t)} - x_b^{(t)}) \quad (13)$$

where  $\beta$  is a given coefficient of the variation,  $x_b^{(t)}$  is the optimal individual position in each current nest, and after the position is updated, there will be :

$$x_i^{(t+1)} = x_i^{(t)} + rand \times (x_j^{(t)} - x_i^{(t)}) \quad (14)$$

where  $x_j^{(t)}$  is a nest near the current nest. In the end, the best nest position in the test value is still recorded as  $x_i^{(t+1)}$ .

The specific steps of the algorithm are shown in Figure 4.

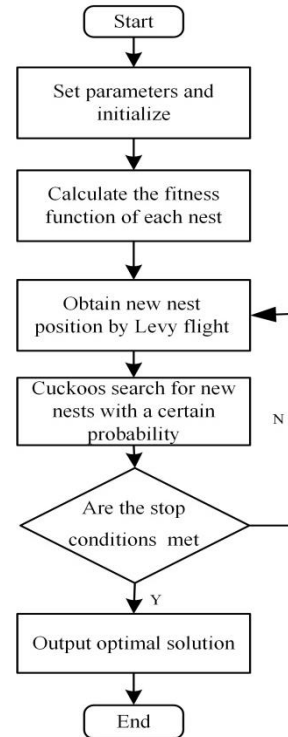


Figure 4. Cuckoo algorithm flow chart.

##### 4.2 PMSA optimal electrifying strategy

The PMSA is driven by an electromagnetic torque. When the stator coil is electrified, the magnetic field is generated, and PM on the rotor ball generates a torque which drives the rotor ball to spin and tilt. If the current flowing into coil  $j$  is  $I_j$ , then the force on the rotor ball is  $F_j$ , which is a tangent to the surface of the rotor ball.

$$F_j = F(I_j, B_r) \quad (15)$$

where  $B_r$  is the radial component of the air-gap flux density. According to the Newton's third law, corresponding torque  $F_j$  on the rotor ball is  $T_j$ .

$$T_j = -F(I_j, B_r) \times r \quad (16)$$

If more than one stator coil is energized, the resultant torque on the rotor ball is:

$$T = \sum_{j=1}^n T_j = -\sum_{j=1}^n F(I_j, B_r) \times r \quad (17)$$

where  $n$  represents the number of the energized coils. The rotor rotation can be expressed as:

$$T = Ja \quad (18)$$

where  $J$  is the moment of inertia and  $a$  is the acceleration. By decomposing it in the Cartesian coordinate system, we get:

$$\begin{cases} T_x = J_x a_x \\ T_y = J_y a_y \\ T_z = J_z a_z \end{cases} \quad (19)$$

It can be seen that when the current is applied to different coils, the generated torque can make the rotor ball move in space.

Due to its structure, PMSA can complete a 3-DOF motion. Spin and tilt are its most typical motions. Figure 5 shows the spin and tilt motion. Any 3-DOF motion can be regarded as a combination of the spin and tilt motion. The PMSA spin and tilt motion are taken as research objects, and the corresponding power on the strategy is formulated.

According to the actual experimental torque, the spin motion only needs to apply a 0.1 Nm torque to the Z axis. The tilt motion is selected to tilt along the Y axis, and a torque of 0.1 Nm is applied to the X axis.

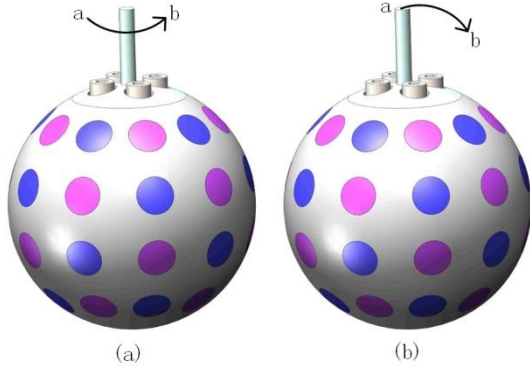


Figure 5. Spin and tilt motion.

For the above two kinds of motion, a point is selected of every degree to calculate the current of the coil. The value of 30 points is needed for both the spin and tilt motion.

For each optimization point, the relationship between a given torque, the torque generated by 24 coils and the current is shown in below formulae:

$$\mathbf{T} = \begin{bmatrix} T_x \\ T_y \\ T_z \end{bmatrix} = \mathbf{A} \cdot \mathbf{I} \quad (20)$$

$$\begin{cases} \mathbf{A} = \begin{bmatrix} T_{x1} & T_{x2} & \dots & T_{x24} \\ T_{y1} & T_{y2} & \dots & T_{y24} \\ T_{z1} & T_{z2} & \dots & T_{z24} \end{bmatrix} \\ \mathbf{I} = [I_1, I_2, \dots, I_{24}]^T \end{cases} \quad (21)$$

where  $\mathbf{T}$  is the moment matrix,  $T_x$ ,  $T_y$  and  $T_z$  represent are the given torque on the X axis, Y axis and Z axis, respectively,  $T_{xi}$ ,  $T_{yi}$ , and  $T_{zi}$  are the components of the torque produced by the unit current of 24 coils at a certain position on the X axis, Y axis and Z axis, respectively obtained by the position torque model of a random forest.  $\mathbf{A}$  is the corner characteristic matrix,  $I_i$  is the current of 24 coils given by the obtained power on the strategy, and  $\mathbf{I}$  is the current matrix of each coil. The torque produced by 24 coils under the unit current and the given torque of the X axis, Y axis and Z axis are known.

Then, according to the optimization point, the cuckoo algorithm is used to optimize the current. Objective function  $Q$  is as follows:

$$Q = \text{Min} \left( \sum_{i=1}^{24} I_i^2 \right) \quad (22)$$

The objective function shows that the copper consumption of the coil is minimal and the energy is the optimal when PMSA is in the motion control mode. For the PSO algorithm, the formula is the fitness function.

For the above objective function, there are the following constraints:

$$\begin{cases} T_{x1}I_1 + T_{x2}I_2 + \dots + T_{x24}I_{24} = T_x \\ T_{y1}I_1 + T_{y2}I_2 + \dots + T_{y24}I_{24} = T_y \\ T_{z1}I_1 + T_{z2}I_2 + \dots + T_{z24}I_{24} = T_z \\ -3 \leq I_i \leq 3 \end{cases} \quad (23)$$

The magnitude of the current flowing into each coil is between  $-3A$  and  $3A$ , and the negative sign indicates that the direction of the current is opposite. The range of the current represents the PSO position interval. Finally, the current values of 24 groups are obtained.

$$\mathbf{I} = [I_1, I_2, \dots, I_{24}]^T \quad (24)$$

Combined with the black box model established by the random forest algorithm, the PIM, PSO and cuckoo algorithm are used to solve the current of the PMSA spin and tilt motion and the results are compared and analyzed. Figures 7 and 8 show comparison results of the sum of squares of the currents for the spin and tilt motion, respectively, in the three algorithms.

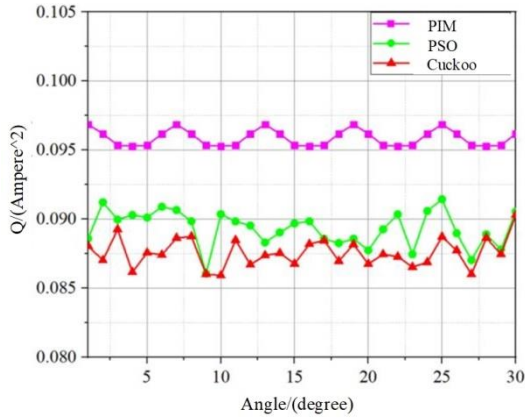


Figure 6. Sum of the squares of the three currents in the spin motion.

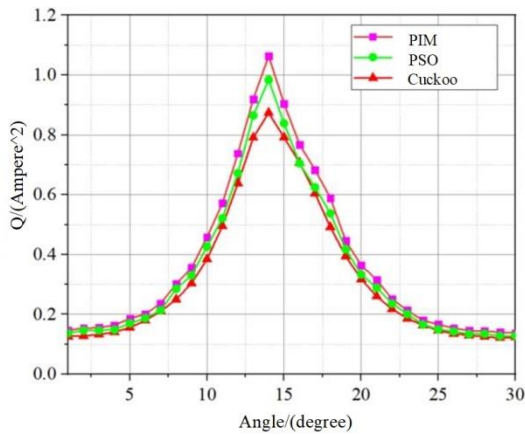


Figure 7. Sum of the squares of the three currents in the tilting motion.

Based on the results of the PIM algorithm used a benchmark, the percentage reduction of the results obtained by the cuckoo and PSO algorithm. The percentage of the power-loss reduction is the optimization rate.

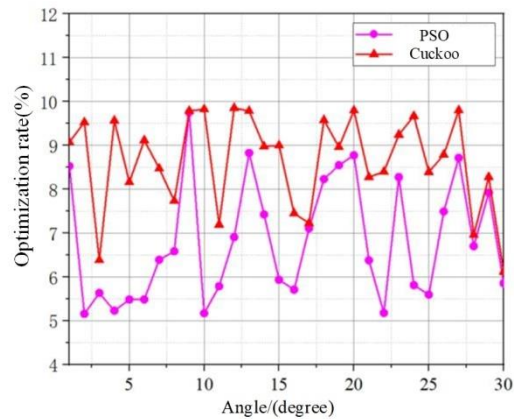


Figure 8. Spin motion optimization rate.

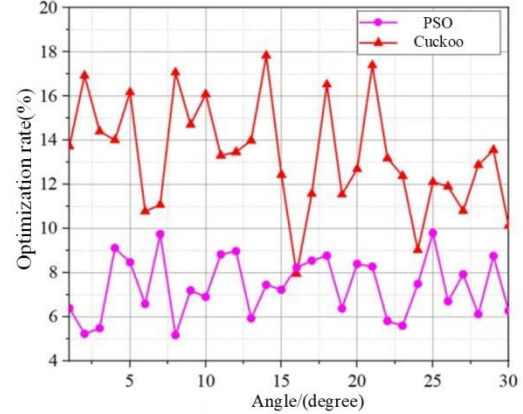


Figure 9. Tilt motion optimization rate.

According to the results in Figures 6 and 7, the cuckoo and PSO algorithm are greatly improved in terms of the spin or tilt motion compared with the traditional PIM algorithm. The results in Figures 8 and 9 show that the optimization rate of the cuckoo and PSO algorithm is 5% - 10%. When solving the tilt motion, the optimization rate of the cuckoo algorithm is 8% - 18% and that of the PSO algorithm is 5% - 10%. It can be seen that the optimization rate of the cuckoo algorithm is higher than that of the PSO algorithm, and there are only a few points that have a lower optimization rate than the PSO algorithm. The possible reason is that the PSO position update process has a direction, so it may fall into the local optimum. However, the cuckoo algorithm uses the Levy's flight and random walk position update, so it will not fall into a trap problem of a local optimum. Therefore, the optimization rate of the cuckoo algorithm is higher than that of the PSO algorithm.

### 5. EXPERIMENT

The PMSA experimental set-up is shown in Figure 10. It is mainly composed of a PMSA prototype, control circuit, power supply and host computer. The control circuit is controlled by an ARM chip. The driving circuit outputs 24 channels of adjustable driving current. The MEMS sensor is mainly used in position detection. The host computer calculates the position current information and sends the calculated current parameters to the ARM control chip to drive PMSA to realize the three degrees of the freedom motion.

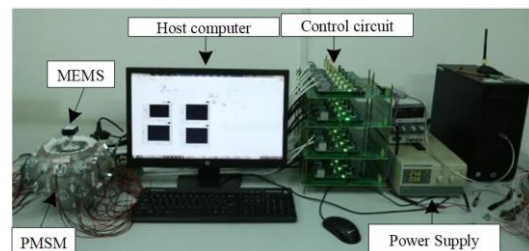


Figure 10. PMSA experimental platform .

According to the simulation results, the overall optimization rate of the cuckoo algorithm is higher than that of the PSO algorithm. The power of the 24 coils corresponding to each point in the PMSA running track is tabulated in the host computer for the experiment. The PMSA position is fed-back to the host computer in real time. Compared with the PIM algorithm, the spin trajectory error curves of the cuckoo algorithm are shown in Figure 11.

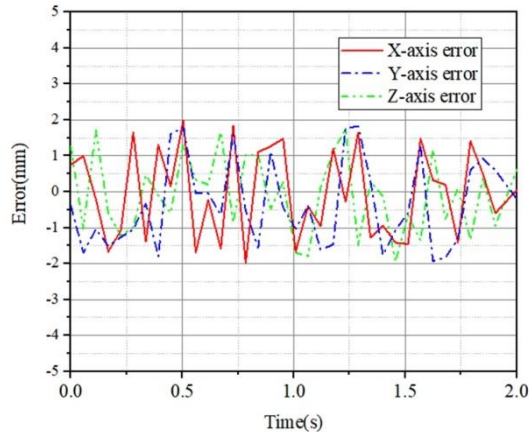


Figure 11. Spin trajectory error curves based on the cuckoo electrifying strategy.

Similarly, compared with the PIM algorithm, the tilt trajectory error curves of the cuckoo algorithm to optimize the power on the strategy are shown in Figure 12.

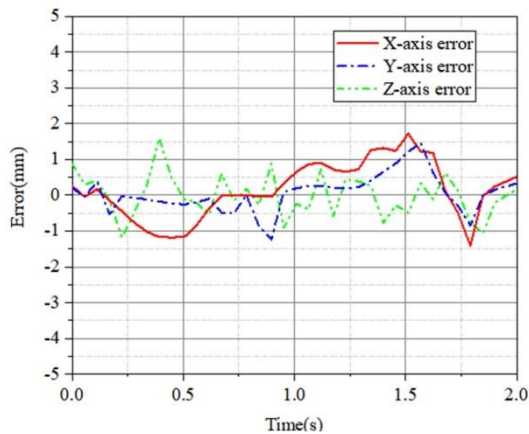


Figure 12. Tilt trajectory error curves based on the cuckoo electrifying strategy.

The experimental results show that the power on the control strategy based on the cuckoo algorithm completes the PMSA spin and tilt motion very well, but according to the error curves, there is still some jitter in the motion process, which may be caused by the friction between the PMSA support structure and the rotor. Compared with the power on the strategy based on the PIM algorithm, the components of the power on the strategy based on the cuckoo algorithm are less than 2 mm on the X axis, Y axis and Z axis. It is proved that

the power on the strategy based on cuckoo algorithm is feasible.

## 6. CONCLUSION

A virtual displacement method is used to obtain the PMSA torque-position data at different positions and a random forest method is used to model the electromagnetic torque characteristics produced by the coils at different positions. Using a model, taking a typical tilt and spin motion as an example, the current values of 24 coils are obtained by solving the PIM and cuckoo algorithm. A comparative analysis of the simulation and experimental results show that the square sum of the current values calculated by the cuckoo algorithm is less than that of the PIM algorithm, which further proves the correctness and feasibility of the proposed cuckoo optimization algorithm.

## ACKNOWLEDGEMENT

The work was financially supported by the National Natural Science Foundation of China (No. 51637001, No. 51307001), the Natural Science Foundation of Anhui Province (2008085ME156), the Young Core Teacher Program of Anhui University (J01005126), and the Academic and Technology Leaders Introduction Project of Anhui University (02303203(32030049)).

## REFERENCES

- [1] Li, Z., Sun, H.Q., Wu, X.L., Liu, Q.R. "Modeling and Levitation Control of a Novel M-DOF Actuator Based on Neural Network", in: International Journal of Applied Electromagnetics and Mechanics, 2012, vol. 38, no. 4, pp. 217-230, ISSN 1383-5416
- [2] Li, Z., Lun, Q., Xing, D., Gao, P. "Analysis and Implementation of a 3-DOF Deflection-Type PM Motor", in: IEEE Transactions on Magnetics, 2015, vol. 51, no. 11, pp. 1-4, ISSN 00189464
- [3] Yan, L., Liu, Y.H., Zhang, L., Jiao, Z.X., Gerada, C. "Magnetic Field Modeling and Analysis of Spherical Actuator with Two-Dimensional Longitudinal Camber Halbach Array", in: IEEE Transactions on Industrial Electronics, 2019, vol. 66, no. 12, pp. 9112-9121, ISSN 0278-0046
- [4] Xia, C.L., Guo, C., Shi, T.N. "A Neural-Network-Identifier and Fuzzy-Controller-Based Algorithm for Dynamic Decoupling Control of Permanent-Magnet Spherical Motor", in: IEEE Transactions on Industrial Electronics, 2010, vol. 57, no. 8, pp. 2868-2878, ISSN 0278-0046
- [5] Zhang, L., Chen, W.H., Liu, J.M., Wen, C.Y. "A Robust Adaptive Iterative Learning Control for Trajectory Tracking of Permanent-Magnet Spherical Actuator", in: IEEE Transactions on Industrial Electronics, 2016, vol. 63, no. 1, pp. 291-301, ISSN 0278-0046
- [6] Liu, J.M., Deng, H.Y., Chen, W.H., Bai, S.P. "Robust Dynamic Decoupling Control for Permanent Magnet Spherical Actuators Based on Extended State Observer", in: IET Control Theory and Applications, 2017, vol. 11, no. 5, pp. 619-631, ISSN 1751-8644
- [7] Liu, J.M., Deng, H.Y., Hu, G.G., Hua, Z.Q., Chen, W.H. "Adaptive Backstepping Sliding Mode Control for 3-DOF Permanent Magnet Spherical Actuator", in: Aerospace Science and Technology, 2017, vol. 67, pp. 62-71, ISSN 1270-9638
- [8] Guo, X.W., Wang, Q.J., Wen, Y., Li, Y.S., Li, S., Zhao, L.J. "Position Tracking Control for a Permanent Magnet Spherical Motor Via Adaptive Fuzzy Backstepping", in: Acta Technica Ceskoslovensk Akademie Ved (CSAV), 2016, vol. 61, no. 4, pp. 397-409, ISSN 00017043

- [9] Guo, X.W., Li, S., Wang, Q.J., Wen, Y., Zhao, L.J. "Continuous Trajectory Planning of Permanent Magnet Spherical Motor by Cubic Spline Interpolation", in: *Electrotehnica, Electronica, Automatica (EEA)*, 2017, vol. 65, no. 3, pp.70-75, ISSN 15825175
- [10] Guo, X.W., Li, S., Wang, Q.J., Zhou, R., Wen, Y. "Analysis of Torque Characteristics and Electrifying Strategy of Permanent Magnet Spherical Motor Based on Triangular Combination Coils", in: *Diangong Jishu Xuebao/Transactions of China Electrotechnical Society*, 2019, vol. 34, no. 8, pp. 1607-1615, ISSN 10006753
- [11] Guo, X.W., Li, S., Wang, Q.J., Wen, Y., Gong, N.W. "Dynamic Analysis and Current Calculation of a Permanent Magnet Spherical Motor for Point-to-Point Motion", in: *IET Electric Power Applications*, 2019, vol. 13, no. 4, pp. 426-434, ISSN 1751-8660
- [12] Park, H.J., Cho, S.Y., Ahn, H.W., Lee, H.J., Won, S.H., Lee, J. "A Study of Advanced Spherical Motor for Improvement of Multi-DOF Motion", in: *Journal of Electrical Engineering & Technology*, 2012, vol.7, no. 6, pp. 926-931, ISSN 0018-9464
- [13] Bai, K., Lee, K.M. "Direct Field-Feedback Control of a Ball-Joint-Like Permanent-Magnet Spherical Motor", in: *IEEE-ASME Transactions on Mechatronics*, 2014, vol. 19, no. 3, pp. 975-986, ISSN 1083-4435
- [14] Nishiura, Y., Hirata, K., Sakaidani, Y., Niguchi, N. "Position Control of 3-DOF Spherical Actuator with Cogging Torque Compensation", in: *International Journal of Applied Electromagnetics and Mechanics*, 2016, vol. 52, no.1-2, pp. 579-589, ISSN 1383-5416
- [15] Zhang, L., Chen, W.H., Liu, J.M., Wu, X.M. "Analysis and Decoupling Control of a Permanent Magnet Spherical Actuator", in: *Review of Scientific Instruments*, 2013, vol. 84, no. 12, pp. 1-11, ISSN 0034-674
- [16] Nguyen, K.D. "On the Adaptive Control of Spherical Actuators", in: *Transactions of the Institute of Measurement and Control*, 2019, vol. 41, no. 3, pp. 816-827, ISSN 0142-3312
- [17] Cracknell, M. J., Reading, A.M. "Geological Mapping Using Remote Sensing Data: A Comparison of Five Machine Learning Algorithms, Their Response to Variations in the Spatial Distribution of Training Aata and the Use of Explicit Spatial Information", in: *Computers and Geosciences*, 2014, vol. 63, pp. 22-33, ISSN 00983004
- [18] Wu, D.Z., Jennings, C., Terenny, J., Gao, R.X., Kumara, S. "A Comparative Study on Machine Learning Algorithms for Smart Manufacturing: Tool Wear Prediction Using Random Forests", in: *Journal of Manufacturing Science and Engineering, Transactions of the ASME*, 2017, vol. 139, no. 7, pp. 1-9, ISSN 10871357
- [19] Mandal, I. "Machine Learning Algorithms for the Creation of Clinical Healthcare Enterprise Systems", in: *Enterprise Information Systems*, 2017, vol. 11, no. 9, pp. 1374-1400, ISSN 17517575
- [20] Li, X.T., Yin, M.H. "Modified Cuckoo Search Algorithm with Self Adaptive Parameter Method", in: *Information Sciences*, 2015, vol. 298, pp. 80-97, ISSN 00200255
- [21] Zhang, Y.W., Wang, L., Wu, Q.D. "Dynamic Adaptation Cuckoo Search Algorithm", in: *Kongzhi yu Juece/Control and Decision*, 2014, vol. 29, no. 4, pp. 617-622, ISSN 10010920
- [22] Abd Elazim, S.M. , Ali, E.S. "Optimal Power System Stabilizers Design Via Cuckoo Search Algorithm", in: *International Journal of Electrical Power and Energy Systems*, 2016, vol. 38, pp. 99-107, ISSN 0142015
- [23] Li, J. "Study of the Optimizing of Physical Distribution Routing Problem Based on Hybrid Cuckoo Algorithm", in: *Energy Education Science and Technology Part A: Energy Science and Research*, 2014, vol. 32, no. 6, pp. 6027-6034, ISSN 1308772X
- [24] Liu, Y.C. "Random Forest Algorithm in Big Data Environment", in: *Computer Modelling and New Technologies*, 2014, vol. 18, no. 12, pp. 147-151, ISSN 14075806
- [25] Abellan, J., Mantas, C.J., Castellano, J.C. "A Random Forest Approach Using Imprecise Probabilities", in: *Knowledge-Based Systems*, 2017, vol. 134, pp. 72-84, ISSN 09507051
- [26] Yang, X. D., S. Cuckoo Search via Levy Flights. *World Congress on Nature and Biologically Inspired Computing*, 2009.

**Xiwen Guo** received his Ph.D. degree in electrical engineering from the Hefei University of Technology, China, in 2012. Currently, he is an associate professor at the School of Electrical Engineering and Automation at the Anhui University of China. His research interest is in special motors and their control, power electronics and electric drives, intelligent control, and motor-pump modelling.

**Siao Wu** graduated from the Bengbu University of China in 2015. He is currently working towards his MS.C. degree at the School of Electrical Engineering and Automation of the Anhui University of China. His research interests include trajectory planning and power on the control strategy of the permanent-magnet spherical actuator.

**Qunjing WANG** received his Ph.D. degree from the University of Science and Technology of China, Hefei, China, in 2001. Currently, he is a professor at the School of Electrical Engineering and Automation at the Anhui University of China. His research interest is in electrical machines, motor drives and novel electric drive systems.

**Guoli Li** received her Ph.D. degree in electrical engineering from ASIPP, Hefei, China, in 2008. Currently, she is a professor at the School of Electrical Engineering and Automation of the Anhui University of China. Her research interest is in electrical & electronic engineering and intelligent optimization techniques.

**Yan Wen** is a Ph.D. candidate in computer application technology at the Anhui University, China. Her research interests include the novel spherical actuator and its control & orientation measurement, complex system modelling and analysis.